# Moveout approximations for P- and SV-waves in dip-constrained transversely isotropic media

Véronique Farra [1] and Ivan Pšenčík [2]

[1]Institut de Physique du Globe de Paris, Sorbonne Paris Cité, Université Paris Diderot, UMR 7154 CNRS, F-75005 Paris, France (farra@ipgp.fr)
[2]Institute of Geophysics, Acad. Sci. of CR, Boční II, 141 31 Praha 4, Czech Republic (ip@ig.cas.cz)

## ABSTRACT

We generalize the P- and SV-wave moveout formulas for transversely isotropic media with vertical axes of symmetry (VTI), based on the weak-anisotropy approximation, for 3D dip-constrained transversely isotropic (DTI) media. A DTI medium is a transversely isotropic medium whose axis of symmetry is perpendicular to a dipping reflector. The formulas are derived in the plane defined by the source-receiver line and the normal to the reflector. In this configuration, they can be easily obtained from the corresponding VTI formulas. It is only necessary to replace the expression for the normalized offset by the expression containing the apparent dip angle. The final results apply to general 3D situations, in which the plane reflector may have arbitrary orientation, and both the source and the receiver may be situated arbitrarily in the DTI medium. The accuracy of the proposed formulas is tested on models with varying dip of the reflector, and for several orientations of the source-receiver line in a horizontal plane.

## INTRODUCTION

Reflection traveltime (moveout) approximations find applications in several branches of processing of reflection data. In most cases, the approximations are based on the Taylor expansion of the square of reflection traveltime $T$ in terms of the square of the source-receiver offset $x$. In anisotropic media, in which the moveout is generally non-hyperbolic, various multiparametric approximations are used (e.g., Aleixo and Schleicher, 2010; Stovas, 2010). Farra and Pšenčík (2013) proposed alternative reflection traveltime formulas for homogeneous VTI media, based on the weak-anisotropy (WA) approximation. Rather than expanding $T^2$ into a Taylor series in terms of $x^2$, they expanded $T^2$ in terms of the weak-anisotropy (WA) parameters, which characterize the deviation of anisotropy from isotropy. The proposed formulas are relatively simple, their complexity slightly increases with the order of approximation. They work well close to the zero-offset and have an exact long-offset asymptote. They may be less accurate for offsets, for which ray- and phase-velocity vectors deviate significantly.

Seismic Waves in Complex 3-D Structures, Report 23, Charles University, Faculty of Mathematics and Physics, Department of Geophysics, Praha 2013, pp. 105–119

Here we generalize the formulas of Farra and Pšenčík (2013) for 3D dip-constrained transversely isotropic (DTI) media, whose symmetry axis is perpendicular to the reflector underlying the transversely isotropic medium. The DTI media are often used in velocity analysis or pre-stack migration. For more details about DTI media, see e.g., Audebert et al. (2006) (who consider DTI as a special case of tilted transverse isotropy), Alkhalifah and Sava (2010, 2011), Golikov et al. (2012). Models with dips can be a reasonable approximation of the complex geological formations such as flanks of salt domes and fold-and-thrust belts (Tsvankin, 2001; Isaac and Lawton, 2004).

We derive the formulas in the plane specified by the source-receiver line and the normal to the reflector. The plane reflector can be situated arbitrarily in a 3D space, the source-receiver line may be oriented arbitrarily in the DTI medium above the reflector except being perpendicular to it. We show that the formulas for the DTI medium can be obtained by a simple generalization of results derived by Farra and Pšenčík (2013) for the VTI case. In fact, it is sufficient to replace the normalized offset $\bar{x}$ used in VTI formulas by the expression $\bar{x}\cos\varphi$, where $\varphi$ denotes the apparent dip angle of the reflector.

We start with the description of the 3D configuration of the reflection experiment, for which we then present the exact traveltime formula and components of the unit vector specifying the ray-velocity direction. In the following sections, we present, successively, P-wave and SV-wave moveout formulas of varying accuracy for DTI media overlying a dipping plane reflector. We also present expressions for the normal moveout (NMO) velocities corresponding to most accurate moveout approximations. The accuracy of the moveout formulas is tested on numerical examples with a varying dip of the reflector, and for several orientations of the source-receiver line situated in a horizontal plane above the reflector.

This paper follows the work of Farra and Pšenčík (2013). In the following, we refer to it as to Paper I. The lower-case indices take the values 1,2,3 and the Einstein summation convention is used.

## SPECIFICATION OF THE MODEL

Let us consider a Cartesian coordinate system $x_i$, $i = 1, 2, 3$, with the $x_3$ axis vertical and positive downwards, and remaining two axes, $x_1$ and $x_2$, situated in the horizontal plane so that the system is right handed. In this coordinate system let us specify an arbitrarily oriented plane reflector $\Sigma$ underlaying a DTI layer, whose axis of symmetry is perpendicular to the reflector $\Sigma$. The reflector $\Sigma$ is specified by the equation:

$$a_i x_i + d = 0 \ . \tag{1}$$

The coefficients $a_i$ represent components of the unit normal $\mathbf{a}$, ($\|\mathbf{a}\| = 1$) to the reflector $\Sigma$. In the DTI layer, we consider two points, $S$ (source) and $R$ (receiver), see the upper plot in Figure 1. The source-receiver line may have an arbitrary orientation except being perpendicular to the reflector $\Sigma$. The offset of points $S$ and $R$ is denoted $x$. The symbol $C$ in Figure 1 denotes the common midpoint, whose orthogonal distance to $\Sigma$ is $H$.

We concentrate first on the plane $\Sigma_a$ defined by the source-receiver line $\overline{SR}$ and the normal to the reflector $\Sigma$, the vector $\mathbf{a}$. The plane $\Sigma_a$ is thus perpendicular to $\Sigma$. The

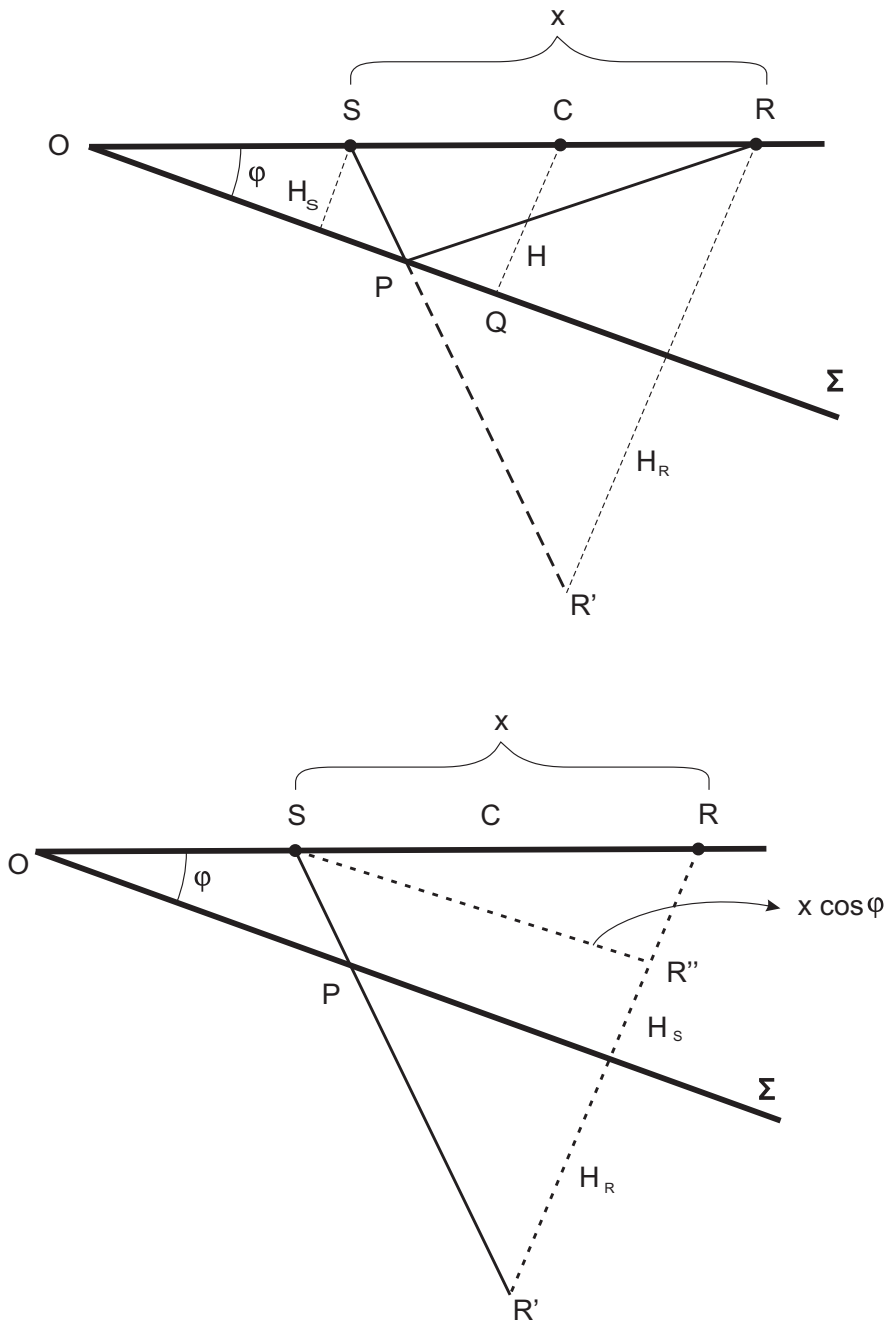


Figure 1: Schematic plot of ray $SPR$ reflected from the dipping reflector $\Sigma$ (top) and the geometry necessary for the derivation of equations 4 and 7. $PR'$ - mirror image, with respect to $\Sigma$, of the reflected part of the ray $SPR$. $H_S$ and $H_R$ - orthogonal distances of points $S$ and $R$ to $\Sigma$, respectively. $C$ - common midpoint.

intersection of $\Sigma_a$ and $\Sigma$ makes an angle $\varphi$ with the line $\overline{SR}$. We call the angle $\varphi$ the *apparent dip* of the reflector since it does not generally represent an actual dip. In fact, the actual dip is not necessary in the following derivations. Knowledge of the normal $\mathbf{a}$ to the reflector $\Sigma$ and the $\overline{SR}$ line is sufficient for the derivations.

The expressions for the offset $x$, the orthogonal distance $H$ of the common midpoint $C$ to the arbitrarily oriented reflector $\Sigma$ and the apparent dip angle $\varphi$ of $\Sigma$ are given in Appendix A. Given the reflector specified by equation 1 and coordinates of points S and R, we can evaluate the presented moveout formulas for an arbitrary 3D configuration.

## TRAVELTIME FORMULA

In the following, we seek the formulas for the square of the traveltime along the ray of an unconverted reflected wave, situated in the plane $\Sigma_a$, see the upper plot in Figure 1. The ray starts from point $S$, it is reflected at point $P$ situated at reflector $\Sigma$ underlaying a homogeneous DTI overburden, and terminates at point $R$. In the upper plot of Figure 1, we also show the mirror image with respect to $\Sigma$ of the reflected part $PR$ of the ray, see the dashed segment $PR'$. The fact that points $S$, $P$ and $R'$ are situated on a line is the consequence of the equality of the angles of reflection and incidence, which, in turn, is caused by the symmetry of the TI medium with respect to the normal to $\Sigma$. The symbols $H$, $H_S$ and $H_R$ denote orthogonal distances to the reflector $\Sigma$ of common midpoint $C$ and points $S$ and $R$, respectively. From the upper plot of Figure 1 we can simply deduce that

$$H_S = H - \frac{x}{2}\sin\varphi \ , \qquad H_R = H + \frac{x}{2}\sin\varphi \ . \tag{2}$$

Here $\varphi$ is the above-introduced apparent dip of the reflector $\Sigma$. We denote the length of the reflected ray $SPR$ (which is equivalent to the length of $SPR'$) as $s$. For $s^2$, we can then find from the triangle $SR'R''$ in the bottom plot of Figure 1:

$$s^2 = (H_S + H_R)^2 + x^2\cos^2\varphi = 4H^2 + x^2\cos^2\varphi \ . \tag{3}$$

The exact expression for the square of the traveltime along the reflected ray $SPR$ is thus given by the expression:

$$T^2(x,\varphi) = \frac{4H^2 + x^2\cos^2\varphi}{v^2(\mathbf{n})} \ . \tag{4}$$

The symbol $v = v(\mathbf{n})$ denotes the ray velocity, which is a function of the direction $\mathbf{n}$ of the slowness vector. In the considered DTI model, $v(\mathbf{n})$ is the same along the down- and upgoing parts of the reflected ray (because the TI axis of symmetry is perpendicular to the reflector $\Sigma$).

Let us introduce the following normalization, which we use to rewrite equation 4:

$$\bar{x} = \frac{x}{2H} \ , \qquad T_0 = \frac{2H}{V} \ . \tag{5}$$

Here $\bar{x}$ is the normalized offset, $V$ is the phase velocity along the symmetry axis, $V = \alpha_0$ in case of P-waves and $V = \beta_0$ in case of SV-waves. Symbols $\alpha_0$ and $\beta_0$ denote P- and SV-wave phase velocities along the axis of symmetry of the DTI medium. Symbol $T_0$

denotes the two-way zero-offset traveltime at the common midpoint $C$. Using equation 5, equation 4 can be expressed as:

$$T^2(\bar{x},\varphi) = V^2 T_0^2 \ \frac{1+\bar{x}^2\cos^2\varphi}{v^2(\mathbf{n})} \ . \tag{6}$$

Note that for zero apparent dip ($\varphi = 0^o$), equation 6 reduces to equation 3 of Paper I.

In order to evaluate $T^2$ in equation 6, it is necessary to determine the direction $\mathbf{n}$ of the slowness vector. It may differ considerably from the direction $\mathbf{N}$ of the ray velocity (the direction of $\overline{SP}$ or $\overline{PR}$ lines in the upper plot of Figure 1), which specifies the direction of the ray. The components of $\mathbf{N}$ can be determined from the geometry shown in the bottom plot of Figure 1. It is not important if $\mathbf{N}$ specifies the direction of the downgoing ($\overline{SP}$) or upgoing ($\overline{PR}$) part of the ray of the reflected wave because the corresponding ray velocity $v(\mathbf{n})$ is the same in both directions. Let us consider the downgoing part $\overline{SP}$. We seek the components of the vector $\mathbf{N}$ in the local Cartesian coordinate system connected with $\Sigma$: $N_3$ is the component of $\mathbf{N}$ along the unit normal $\mathbf{a}$ to $\Sigma$, positive downwards, $N_1$ is the component of $\mathbf{N}$ to the reflector $\Sigma$, positive to the right. Using the triangle $SR'R''$ in the bottom plot of Figure 1, we can find that $N_1 = x\cos\varphi/s$ and $N_3 = 2H/s$, which, after using equations 3 and 5, yields:

$$N_1 = \frac{\bar{x}\cos\varphi}{\sqrt{1+\bar{x}^2\cos^2\varphi}} \ , \qquad N_3 = \frac{1}{\sqrt{1+\bar{x}^2\cos^2\varphi}} \ . \tag{7}$$

For $\varphi = 0^o$, equation 7 yields equation 4 of Paper I.

When comparing equations 6 and 7 with their counterparts in Paper I, which were derived for $\varphi = 0^o$, we can see that we can obtain equations 6 and 7 by replacing $\bar{x}$ in formulas derived in Paper I by $\bar{x}\cos\varphi$. We have expressed the components of vector $\mathbf{N}$ in the local Cartesian coordinate system, in which one axis, perpendicular to $\Sigma$, is parallel to the symmetry axis of the TI medium. We can thus use the expressions for the phase and ray velocities and other auxiliary expressions derived for the VTI case in Paper I, for the generalization of the approximate moveout formulas to the DTI case.

We can see that the introduction of the apparent dip in DTI media leads to stretching of the normalized offset axis. The larger the apparent dip the greater the stretch. This is true not only for exact expression 6, but also for all approximate expressions derived in this paper.

Due to the existence of the apparent dip, only finite offsets can be considered. While in the VTI media (zero dip), the offset can be infinite, in the DTI media, the maximum offset is finite. The maximum normalized offset $\bar{x}_{MAX}$ is $\bar{x}_{MAX} = 1/\sin\varphi$, as simply follows from the triangle OQC in the upper plot of Figure 1.

The moveout formulas depend, in addition to the normalized offset $\bar{x}$ and the apparent dip angle $\varphi$, on the weak-anisotropy (WA) parameters $\epsilon_W$, $\delta_W$ and $\sigma_W$. They are defined as $\epsilon_W = (A_{11} - \alpha_0^2)/2\alpha_0^2$, $\delta_W = (A_{13} + 2A_{55} - \alpha_0^2)/\alpha_0^2$ and $\sigma_W = r^{-2}(\epsilon_W - \delta_W)$, where $r = \beta_0/\alpha_0$. The parameters $\epsilon_W$ and $\delta_W$ represent linearized Thomsen's (1986) VTI parameters $\epsilon$ and $\delta$. Note that $\epsilon_W = \epsilon$. Parameter $\sigma_W$ is a linearized version of parameter $\sigma$, see Tsvankin (2001). Symbols $A_{\beta\gamma}$ ($\beta,\gamma = 1,2,...,6$) denote density-normalized elastic moduli in the Voigt notation. Both WA parameters and elastic moduli are specified in

the local Cartesian coordinate system, two axes of which are situated in $\Sigma$ and the third is perpendicular to $\Sigma$, i.e., parallel to the axis of symmetry of the DTI medium. Since $\alpha_0$ and $\beta_0$ are phase velocities along the symmetry axis, we have $\alpha_0^2 = A_{33}$, $\beta_0^2 = A_{55}$. Finally, through the two-way zero-offset traveltime $T_0$, the moveout formulas also depend on the orthogonal distance $H$ of common midpoint $C$ to the reflector $\Sigma$, and thus on the position of $C$.

## P-WAVE MOVEOUT

Let us specify $V = \alpha_0$ and ignore the difference between vectors $\mathbf{n}$ and $\mathbf{N}$. Then in the first-order approximation, $v^2(\mathbf{n}) = c^2(\mathbf{N})$, where $c(\mathbf{N})$ is the phase velocity in the ray direction, and we obtain from formula 6 and formulas of Paper I the first-order expression for $T^2$:

$$T^2(\bar{x},\varphi) = T_0^2 \frac{(1+\bar{x}^2\cos^2\varphi)^3}{P(\bar{x},\varphi)} \ . \tag{8}$$

Here

$$P(\bar{x},\varphi) = (1+\bar{x}^2\cos^2\varphi)^2 + 2\delta_W\bar{x}^2\cos^2\varphi + 2\epsilon_W\bar{x}^4\cos^4\varphi \ . \tag{9}$$

For zero apparent dip, $\varphi = 0^o$, equations 8 and 9 reduce to equations 20 and 21, respectively, of Paper I.

If we take into account the difference between vectors $\mathbf{n}$ and $\mathbf{N}$ and between phase and ray velocities squared, we obtain a more accurate first-order expression for $T^2$:

$$T^2(\bar{x},\varphi) = T_0^2 \frac{(1+\bar{x}^2\cos^2\varphi)^3 P(\bar{x},\varphi)}{P^2(\bar{x},\varphi) - Q^2(\bar{x},\varphi)} \ . \tag{10}$$

Polynomial $P(\bar{x},\varphi)$ is given in equation 9 and $Q(\bar{x},\varphi)$ reads:

$$Q(\bar{x},\varphi) = 2\bar{x}\cos\varphi[2\epsilon_W\bar{x}^2\cos^2\varphi + \delta_W(1-\bar{x}^2\cos^2\varphi)] \ . \tag{11}$$

For $\varphi = 0^o$, equations 10, 9 and 11 reduce to equations 24, 21 and 25, respectively, of Paper I. Polynomial $P(\bar{x},\varphi)$ contains terms of zero and first order in the WA parameters while polynomial $Q(\bar{x},\varphi)$ contains only terms of the first order. Thus if we wish to ignore the second-order terms in the WA parameters in equation 10, $Q^2(\bar{x},\varphi)$ must be neglected with respect to $P^2(\bar{x},\varphi)$, and equation 10 reduces to equation 8. Note that polynomials $P(\bar{x},\varphi)$ and $Q(\bar{x},\varphi)$ can be obtained from their counterparts in Paper I by replacing $\bar{x}$ from Paper I by $\bar{x}\cos\varphi$.

The accuracy of formula 10 can be further increased by using the more accurate expression for the ray velocity. In this way we obtain the second-order expression for $T^2$:

$$T^2(\bar{x},\varphi) = T_0^2 \frac{(1+\bar{x}^2\cos^2\varphi)^3 P(\bar{x},\varphi)}{P^2(\bar{x},\varphi) + aQ^2(\bar{x},\varphi)} \ . \tag{12}$$

Here $a = (r^2 - 3/4)/(1-r^2)$, where $r = \beta_0/\alpha_0$. For $\varphi = 0^o$, equations 12, 9 and 11 reduce to equations 26, 21 and 25, respectively, of Paper I.

As in the VTI case studied in Paper I, the above formulas yield NMO velocities $v^W_{NMO}$, whose accuracy depends on the accuracy of the corresponding moveout formula. The most accurate expression can be obtained from equation 12. It reads:

$$(v^W_{NMO})^2 = \alpha_0^2[(1 - 2\delta_W - 4a\delta_W^2)\cos^2\varphi]^{-1} \ , \tag{13}$$

where $a$ is defined after formula 12. Equation 13 represents the second-order approximation of the square of the exact NMO velocity for a dipping reflector: $v^2_{NMO} = \alpha_0^2(1 + 2\delta)/\cos^2\varphi$. Here $\delta$ is the Thomsen's (1986) parameter. In the derivation of expression 13 from the corresponding expression in Paper I, we used the above-mentioned fact that the DTI formulas follow from the VTI ones when we replace $\bar{x}$ by $\bar{x}\cos\varphi$. We can see that in DTI media, as in isotropic media, the NMO velocity corresponding to a dipping reflector differs from its zero-dip counterpart by the multiplicative factor $1/\cos\varphi$ (Levin, 1971; Grechka, 2009).

## SV-WAVE MOVEOUT

In the following, we consider the S-wave polarized in the plane $\Sigma_a$ and denote it SV-wave.

Let us specify $V = \beta_0$ and ignore the difference between vectors $\mathbf{n}$ and $\mathbf{N}$. Then, in the first-order approximation, $v^2(\mathbf{n}) = c^2(\mathbf{N})$, where $c(\mathbf{N})$ is the phase velocity in the ray direction, and we can write the first-order expression for $T^2$ in the form:

$$T^2(\bar{x},\varphi) = T_0^2\frac{(1 + \bar{x}^2\cos^2\varphi)^3}{P(\bar{x},\varphi)} \ . \tag{14}$$

In equation 14, $P(\bar{x},\varphi)$ is polynomial, which reads:

$$P(\bar{x},\varphi) = (1 + \bar{x}^2\cos^2\varphi)^2 + 2\sigma_W\bar{x}^2\cos^2\varphi \ , \tag{15}$$

where $\sigma_W = r^{-2}(\epsilon_W - \delta_W)$. For $\varphi = 0^o$, equations 14 and 15 reduce to equations 41 and 42, respectively, of Paper I.

If we take into account the difference between vectors $\mathbf{n}$ and $\mathbf{N}$ and between phase and ray velocities, we can obtain a more accurate first-order expression for $T^2$:

$$T^2(\bar{x},\varphi) = T_0^2\frac{(1 + \bar{x}^2\cos^2\varphi)^3 P(\bar{x},\varphi)}{P^2(\bar{x},\varphi) - Q^2(\bar{x},\varphi)} \ . \tag{16}$$

In formula 16, polynomial $P(\bar{x},\varphi)$ is given in equation 15 and $Q(\bar{x},\varphi)$ reads:

$$Q(\bar{x},\varphi) = 2\sigma_W\bar{x}\cos\varphi(1 - \bar{x}^2\cos^2\varphi) \ . \tag{17}$$

Again, for $\varphi = 0^o$, equations 16, 15 and 17 reduce to equations 45, 42 and 46, respectively, of Paper I. Polynomial $P(\bar{x},\varphi)$ contains terms of zero and first order in the WA parameters while polynomial $Q(\bar{x},\varphi)$ contains only terms of the first order. Thus if we wish to ignore the second-order terms in the WA parameters in equation 16, $Q^2(\bar{x},\varphi)$ must be neglected with respect to $P^2(\bar{x},\varphi)$, and formula 16 reduces to formula 14.

The accuracy of formula 16 can be further increased by using the more accurate expression for the ray velocity. In this way, we obtain the second-order expression for $T^2$:

$$T^2(\bar{x},\varphi) = T_0^2 \frac{(1+\bar{x}^2\cos^2\varphi)^3 P(\bar{x},\varphi)}{P^2(\bar{x},\varphi) - Q^2(\bar{x},\varphi) - br^2R^2(\bar{x},\varphi)} \ . \tag{18}$$

Here $R(\bar{x},\varphi)$ reads:

$$R(\bar{x},\varphi) = r^{-1}\bar{x}\cos\varphi[2\epsilon_W\bar{x}^2\cos^2\varphi + \delta_W(1-\bar{x}^2\cos^2\varphi)] \tag{19}$$

and $b = r^{-2}(1-r^2)^{-1}$. For $\varphi = 0^o$, equations 18, 15, 17 and 19 reduce to equations 47, 42, 46 and 48 of Paper I. We can see that $R(\bar{x},\varphi)$ contains only first-order terms with respect to the WA parameters. Thus if we wish to neglect the second-order terms in formula 18, it reduces to formula 14 again.

Polynomials $P(\bar{x},\varphi)$, $Q(\bar{x},\varphi)$ and $R(\bar{x},\varphi)$ can again be obtained from their counterparts in Paper I by replacing $\bar{x}$ from Paper I by $\bar{x}\cos\varphi$.

Similarly as in the P-wave case, we can transform the formula for the NMO velocity in the VTI media in Paper I, corresponding to the second-order SV-wave moveout expression, into the form for the DTI media. We get:

$$(v_{NMO}^W)^2 = \beta_0^2[(1-2\sigma_W+4\sigma_W^2+b\delta_W^2)\cos^2\varphi]^{-1} \ , \tag{20}$$

where $b$ is defined after equation 19. Equation 20 represents the second-order approximation of the square of the exact SV-wave NMO velocity for a dipping reflector: $v_{NMO}^2 = \beta_0^2(1+2\sigma)/\cos^2\varphi$, with $\sigma = r^{-2}(\epsilon-\delta)$, $\epsilon$ and $\delta$ being Thomsen's (1986) non-linearized parameters. The difference between $\sigma$ and its linearized counterpart, $\sigma_W$, is the reason why equation 20 contains, in addition to $\sigma_W$, also $\delta_W$.

## NUMERICAL TESTS

As mentioned in the text, the dip of the reflector causes stretching of the normalized offset axis in plots of $T^2 = T^2(\bar{x})$ curves. As a consequence, these curves can be easily obtained from those derived in Paper I for the VTI medium ($\varphi = 0^o$). Thus the results of the comparisons of their accuracy with commonly used moveout formulas performed in Paper I apply also to the formulas presented in this paper. For this reason, we concentrate here only on tests of accuracy of the DTI formulas for varying dips of the reflector $\Sigma$ and for varying direction of the source-receiver line with respect to the dipping reflector. We model the dipping plane reflectors so that their normals $\mathbf{a}$ are always situated in the plane $(x_1, x_3)$, i.e., the $x_1$-axis represents the dip direction. Although the formulas in the preceding sections hold for an arbitrary orientation of the source-receiver line except perpendicular to $\Sigma$ (then the plane $\Sigma_a$ is not defined), we consider only horizontal source-receiver lines in the following tests. We specify them by the azimuth $A$ measured from the $x_1$-axis. The source-receiver line parallel to the $x_1$-axis has zero azimuth, $A = 0^o$, the line along the strike (the $x_2$-axis) has the azimuth $A = 90^o$. In the former case, the apparent dip, $\varphi$, equals the actual dip, $\varphi_a$. In the latter case, the apparent dip is zero. This is confirmed by the following equation relating the apparent and actual dips and the azimuth:

$$\sin\varphi = \sin\varphi_a\cos A \ . \tag{21}$$

Equation 21 follows from simple geometrical considerations or directly from equation A-3, taking into account the above definition of the azimuth $A$. In the following tests, we use formula 21 and parameterize the plots by the actual dip $\varphi_a$ and the azimuth $A$ of the source-receiver line.

We test the proposed formulas, specifically formulas 8 and 12 for P-waves and formulas 14 and 18 for SV-waves. We present plots of the relative errors $(T - T_{ex})/T_{ex} \times 100\%$, where $T$ is the approximate traveltime obtained from the above-mentioned formulas and $T_{ex}$ denotes the traveltime calculated using the package ANRAY (Gajewski and Pšenčík, 1990), which we take as an exact reference. Because $T$ and $T_{ex}$ depend linearly on $T_0$, the relative errors are independent of $T_0$. It means that the relative errors are also independent of the position of the common midpoint $C$ and, thus, of the depth $H$ of the reflector $\Sigma$ under it. The anisotropy strength is defined as $2(V_{max} - V_{min})/(V_{max} + V_{min}) \times 100\%$. The models considered are the Greenhorn shale model with a P-wave anisotropy of $\sim$ 26% and the limestone model, whose SV-wave anisotropy is $\sim$ 5%. The parameters of both models are given in Table 1.

| Model | $\alpha_0$(km/s) | $\beta_0$(km/s) | $\epsilon_W$ | $\delta_W$ |
|---|---|---|---|---|
| Limestone | 3.0 | 1.707 | 0.076 | 0.133 |
| Greenhorn shale | 3.094 | 1.51 | 0.256 | -0.0523 |

Table 1: Parameters of the models used. $\alpha_0$ and $\beta_0$ - P- and S-wave velocities along the axis of symmetry, $\epsilon_W$ and $\delta_W$ - WA parameters referenced to the axis of symmetry.

Figures 2 and 3 have the same structure. The plots in each column correspond, from the top to the bottom to the azimuths of the source-receiver line varying from $0^o$ to $90^o$ with the step of $30^o$. Each plot, except the lowest, contains six curves, corresponding to the actual dips, $\varphi_a$, of $0^o$ (black), $15^o$ (red), $30^o$ (blue), $45^o$ (green), $60^o$ (violet) and $75^o$ (yellow). The lowest plots contain only one curve because in this case, the apparent dip is zero (no matter how large the actual dip is) and, thus, the plots represent, in fact, results corresponding to the VTI case. They correspond to the results presented in Paper I and to the black curves in the uppermost plots (for $A = 0^o$). The length of the colored curves varies with the maximum normalized offset $\bar{x}_{MAX}$ for each dip. The longest are the black curves ($\bar{x}_{MAX}$ is infinite) corresponding to the zero dip, the shortest are the yellow curves corresponding to the dip of $75^o$.

Figure 2 shows the relative traveltime errors of P-wave formulas 8 (left) and 12 (right) for the Greenhorn shale model. The black curves in the uppermost and lowest plots correspond to the red curve (left) and the blue curve (right) in Figure 2d of Paper I. As expected, equation 8 (left), which ignores the difference between the directions of **N** and **n**, yields worse results. The maximum relative errors are around 2.5 %. When the deviations of **N** and **n** are taken into account and when the second-order equation 12 is used (right), the maximum relative errors are reduced below 0.6 %. The effects of varying dips of $\Sigma$ and azimuth $A$ are generally small. They are, of course, more pronounced for smaller azimuths. For a fixed normalized offset, the errors of both formulas 8 and 12 slightly increase or decrease with increasing dip $\varphi$, depending on the character of the curves of traveltime relative errors. This is an effect of the $\cos\varphi$ factor in the moveout formulas.

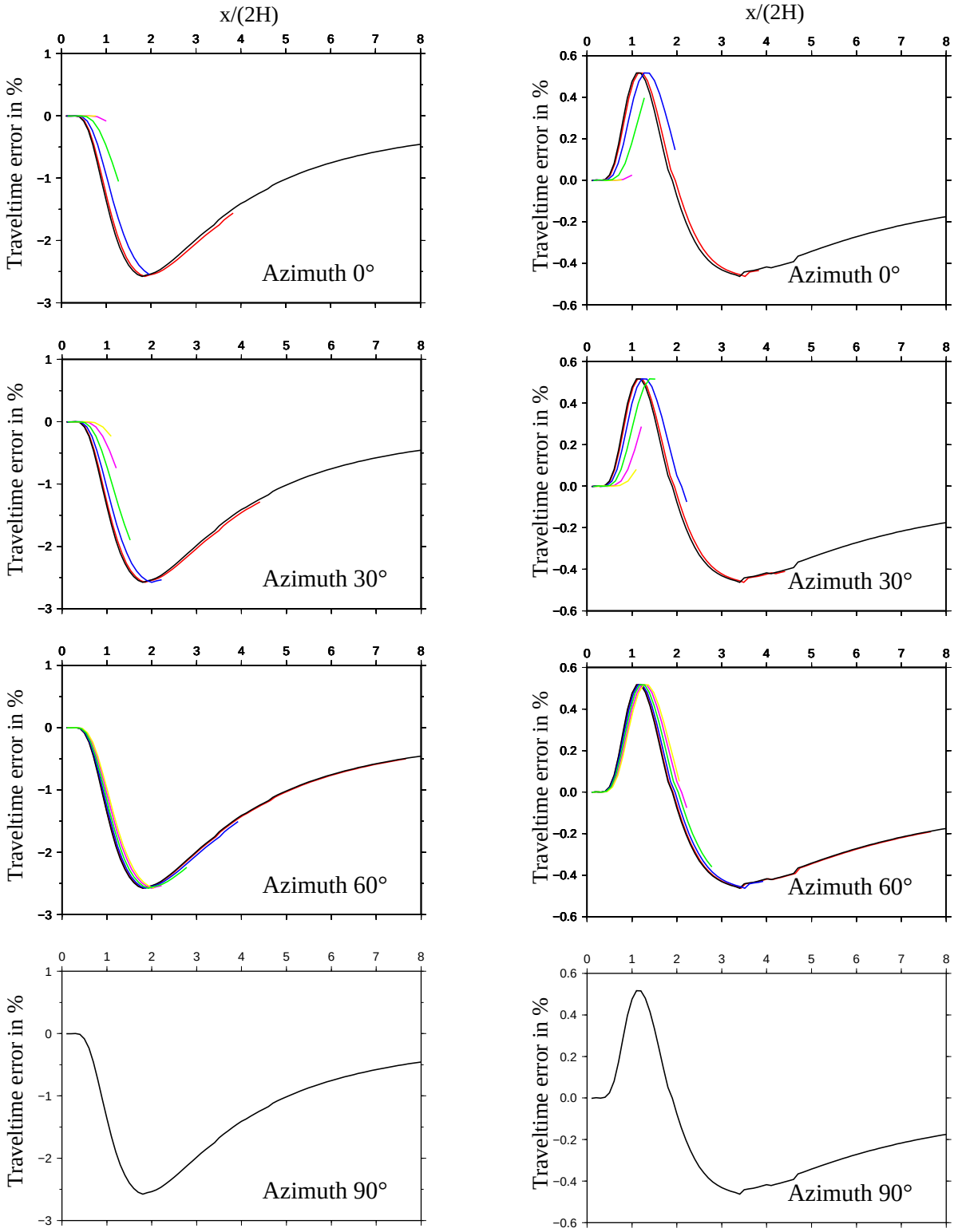


Figure 2: P-wave moveout in the Greenhorn shale model, anisotropy $\sim 26\%$. Variation with the normalized offset $\bar{x} = x/2H$ of relative traveltime errors of the first-order equation 8 ignoring difference in directions of vectors $\mathbf{N}$ and $\mathbf{n}$ (left column) and of second-order equation 12 (right column). The source-receiver lines are in the horizontal plane; their azimuths ($0^o$, $30^o$ $60^o$ and $90^o$) are measured from the dip direction ($x_1$-axis). The colored curves correspond to varying actual dips of the reflector $\Sigma$: dip $0^o$ - black, $15^o$ - red, $30^o$ - blue, $45^o$ - green, $60^o$ - violet, $75^o$ - yellow.

Figure 3 shows the relative traveltime errors of SV-wave formulas 14 (left) and 18 (right) for the limestone model. The black curves in the uppermost and lowest plots correspond to the red curve (left) and the blue curve (right) in Figure 3d of Paper I. Here, however, the scales of the vertical axes are significantly different. Due to more detailed scales, the curves have a noisy character, which is caused by the two-point ray tracing procedure used for the reference traveltime computations in the package ANRAY. The approximate traveltime curves are smooth. The maximum relative errors are in this case smaller than in Figure 2. For the formula 14, their maximum value is about 0.85 %, for the formula 18 less than 0.2 %. In both cases, for increasing offsets, the errors decrease. The effects of varying dips of $\Sigma$ and azimuth $A$ are again generally small.

For completeness, we present here also exact and approximate values of NMO velocities for the two models shown in Figures 2 and 3. The values correspond to $A = 0^o$ and $\varphi_a = 0^o$. For the Greenhorn shale model, the exact value is 2.934 km/s. The first-order formula (not shown here) yields 2.944 km/s and the second-order formula 13 yields the exact value, i.e., 2.934 km/s. For the limestone model, the exact value is 1.286 km/s. The first-order formula (again not shown here) yields 1.468 km/s and the second-order formula 20 yields 1.368 km/s. We can see that the errors of the approximate NMO velocities are larger for SV wave. Let us remark that the relative difference between exact NMO velocity and phase velocity along the symmetry axis (Table 1) is much larger for SV-wave (28%) in the limestone model than for P-wave (5.3%) in the Greenhorn model.

## CONCLUSIONS

We have shown that the moveout P-wave and SV-wave formulas for the dip-constrained transversely isotropic media can be easily derived from those for the VTI media, see Paper I. It is only necessary to specify vector $\mathbf{N}$ and the WA parameters in the local Cartesian coordinate system connected with the dipping reflector $\Sigma$. We showed that we can then use the formulas derived in Paper I and replace the normalized offset $\bar{x}$ in them by $\bar{x}\cos\varphi$ to obtain the corresponding DTI formulas.

The replacement of the normalized offset $\bar{x}$ by $\bar{x}\cos\varphi$ leads to a stretch of the normalized offset axis. The stretch increases with the increasing dip of the reflector. When the traveltime errors for the VTI media ($0^o$ dip) increase (decrease) with offset, the existence of the dip causes a slight decrease (increase) of the error for a given offset. This can be observed in Figures 2 and 3. The effects of the dip are, however, generally quite small.

The presented moveout formulas depend on the normalized offset $\bar{x}$, the apparent dip angle $\varphi$ and the WA parameters $\epsilon_W$, $\delta_W$ and $\sigma_W$, see Paper I for more details. The WA parameters are referenced to the axis of symmetry, which is perpendicular to the dipping reflector $\Sigma$. The moveout formulas depend on the position of the common midpoint $C$ and the depth $H$ of the reflector $\Sigma$ under it, but the presented relative errors do not.

While the normalized offsets considered in Paper I could run to infinity, the normalized offsets for DTI media have only a limited extent, $\bar{x}_{MAX} = 1/\sin\varphi$. The larger the dip, the shorter the maximum offset. Of course, the traveltimes calculated from the presented formulas are reciprocal, i.e., for a given common midpoint and offset, it does not matter if the traveltime is calculated from $S$ to $R$ or vice versa.

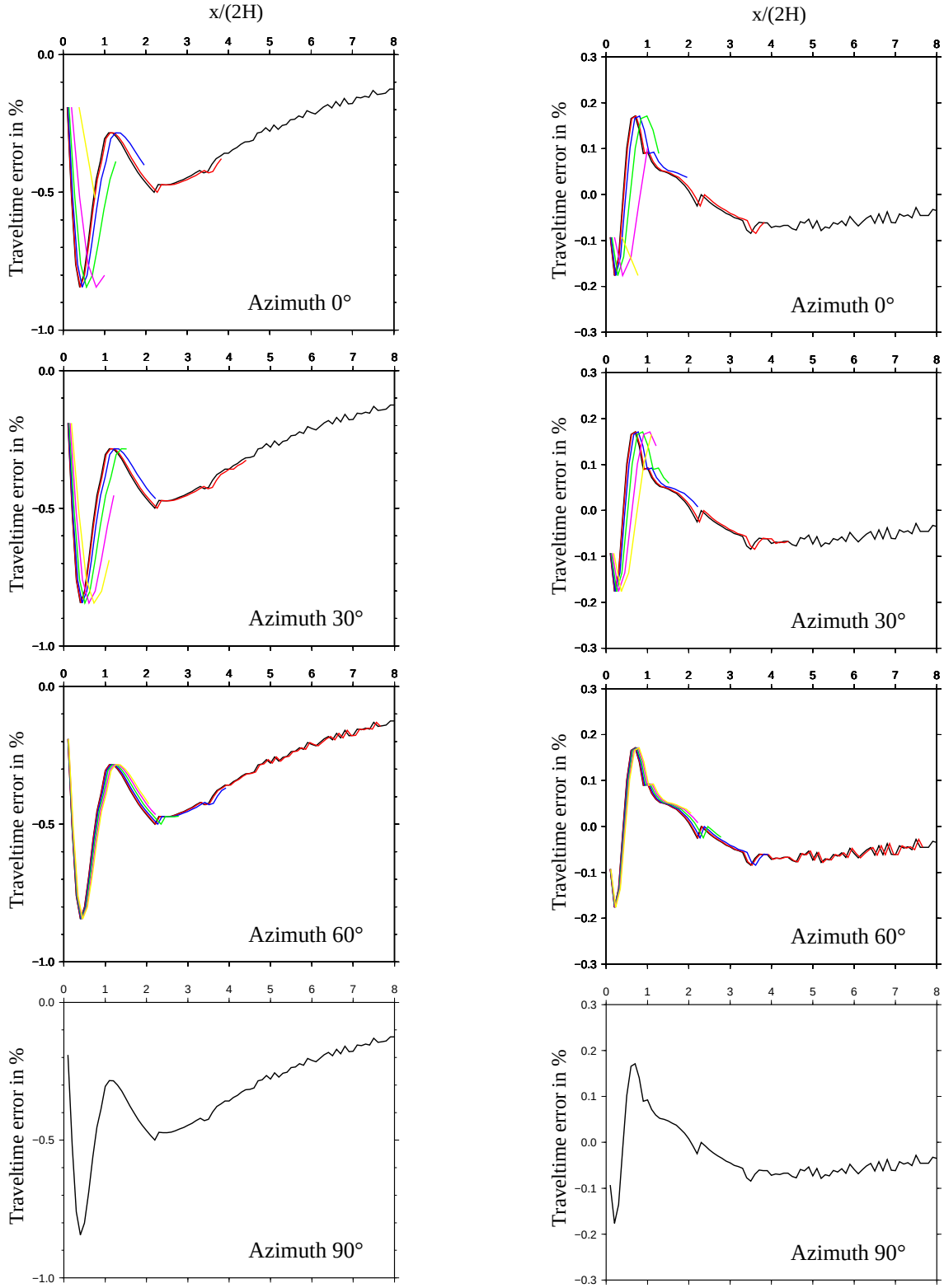


Figure 3: SV-wave moveout in limestone model, anisotropy $\sim 5\%$. Variation with the normalized offset $\bar{x} = x/2H$ of relative traveltime errors of the first-order equation 14 ignoring difference in directions of vectors $\mathbf{N}$ and $\mathbf{n}$ (left column) and of second-order equation 18 (right column). The source-receiver lines are in the horizontal plane; their azimuths ($0^o$, $30^o$ $60^o$ and $90^o$) are measured from the dip direction ($x_1$-axis). The colored curves correspond to varying actual dips of the reflector $\Sigma$: dip $0^o$ - black, $15^o$ - red, $30^o$ - blue, $45^o$ - green, $60^o$ - violet, $75^o$ - yellow.

As shown in numerical tests, the presented formulas can be applied to very general 3D configurations, in which an arbitrary dip of the reflector $\Sigma$ and an arbitrary orientation of the source-receiver line, except being perpendicular to $\Sigma$, can be considered. The expressions for the determination of the offset $x$, the orthogonal distance of the common midpoint to the reflector $\Sigma$ and the apparent dip angle for an arbitrary 3D configuration can be found in Appendix A. The only conditions of applicability of the presented formulas are that the normal to the reflector coincides with the axis of symmetry of the overlying DTI medium, the source-receiver line is situated in this medium, and is not perpendicular to the reflector.

## ACKNOWLEDGEMENTS

We are grateful to Alexey Stovas, Pavel Golikov, Tijmen Jan Moser, Madhav Vyas and the AE, Ian Moore, for constructive and stimulating reviews. Comments of an anonymous reviewer are also appreciated. A substantial part of this work was done during IP′s stay at the IPG Paris at the invitation of the IPGP. We are grateful to the Consortium Project "Seismic waves in complex 3-D structures" (SW3D) and the Research Project 210/11/0117 of the Grant Agency of the Czech Republic for support. The paper has been submitted to Geophysics.

# REFERENCES


Aleixo, R., and J. Schleicher, 2010, Traveltime approximations for q-P waves in vertical transversely isotropy media: Geophys. Prosp., **58**, 191–201.

Alkhalifah, T., and P. Sava, 2010, A transversely isotropic medium with a tilted symmetry axis normal to the reflector: Geophysics, **75**, A19-A24.

Alkhalifah, T., and P. Sava, 2011, Migration using a transversely isotropic medium with symmetry normal to the reflector dip: International Journal of Geophysics, **2011**, Article ID 530106, 1-5.

Audebert, F., V. Dirks, and A. Pettenati, 2006, TTI anisotropic depth migration: What tilt estimate should we use?: SEG Technical Program Expanded Abstracts, **25**, 2382-2386.

Isaac, J. H., and D. C. Lawton, 2004, A practical method for estimating effective parameters of anisotropy from reflection seismic data: Geophysics, **69**, 681-689.

Farra, V., and I. Pšenčík, 2013, Moveout approximations for P- and SV-waves in VTI media: Geophysics, in print.

Gajewski, D., and I. Pšenčík, 1990, Vertical seismic profile synthetics by dynamic ray tracing in laterally varying layered anisotropic structures: J. Geophys. Res., **95**, 11301–11315.

Golikov, P, T. Alkhalifah and A. Stovas, 2012, Prestack traveltimes for dip-constrained TI media: 82nd Annual International Meeting, SEG, Expanded Abstracts, doi: 10.1190/segam2012-0507.1.

Grechka, V., 2009, Applications of seismic anisotropy in the oil and gas industry. EAGE Publications.

Korn, G.A, and Korn, T.M., 1961, Mathematical Handbook for Scientists and Engineers. London, McGraw-Hill.

Levin, F.K., 1971, Apparent velocity from dipping interface reflections: Geophysics, **36**, 510–516.

Stovas, A., 2010, Generalized moveout approximation for qP- and qSV-waves in a homogeneous transversely isotropic medium: Geophysics, **75**, D79–D84.

Thomsen, L., 1986, Weak elastic anisotropy: Geophysics, **51**, 1954–1966.

Tsvankin, I., 2001, Seismic signatures and analysis of reflection data in anisotropic media. Oxford, Elsevier Science Ltd.

# APPENDIX A
# SPECIFICATION OF $x$, $H$ AND $\varphi$ FOR ARBITRARILY ORIENTED $\Sigma$

Here we show how to express the offset $x$, the orthogonal distance $H$ of midpoint $C$ to the reflector $\Sigma$ and the apparent dip $\varphi$ in terms of the parameters specifying the reflector plane $\Sigma$ in global Cartesian coordinates in 3D space, see equation 1. The offset $x$ is the distance of points $S = S(x_i^S)$ and $R = R(x_i^R)$. It is given by a simple formula:

$$x = \sqrt{(x_i^R - x_i^S)(x_i^R - x_i^S)} \; . \qquad (A-1)$$

The orthogonal distance $H$ of the midpoint $C = C(x_i^C)$ to the plane reflector $\Sigma$ specified by equation 1 is:

$$H = a_i x_i^C + d \; , \qquad (A-2)$$

where $d$ is the orthogonal distance of the origin of coordinates to the reflector $\Sigma$. See, for example, Korn and Korn (1961). The same textbook also offers the expression for the apparent dip angle $\varphi$, made by the line $\overline{SR}$ and the intersection of the planes $\Sigma$ and $\Sigma_a$:

$$\sin\varphi = \frac{a_i(x_i^R - x_i^S)}{\sqrt{(x_k^R - x_k^S)(x_k^R - x_k^S)}} \; . \qquad (A-3)$$

The above formulas allow the application of the moveout formulas for the plane reflector $\Sigma$ arbitrarily chosen in 3D space and for points $S$ and $R$ situated anywhere (the line $\overline{SR}$ should not be perpendicular to $\Sigma$) in the DTI layer overlying $\Sigma$.